HHS Public Access

Author manuscript

J Proteomics. Author manuscript; available in PMC 2023 September 08.

Published in final edited form as:

J Proteomics. 2020 September 30; 228: 103939. doi:10.1016/j.jprot.2020.103939.

Dynamics of protein synthesis in the initial steps of strobilation in the model cestode parasite *Mesocestoides corti* (syn. *vogae*)

Jeferson Camargo de Lima[a,b], **Maiara Anschau Floriani**[b,1], **João Antônio Debarba**[a,c,2], **Gabriela Prado Paludo**[a,b], **Karina Mariante Monteiro**[a,b,c], **Hercules Moura**[d], **John R. Barr**[d], **Arnaldo Zaha**[a,c], **Henrique Bunselmeyer Ferreira**[a,b,c,*]

[a]Programa de Pós-Graduação em Biologia Molecular e Celular, Centro de Biotecnologia, Universidade Federal do Rio Grande do Sul (UFRGS), Brazil

[b]Laboratório de Genômica Estrutural e Funcional, Centro de Biotecnologia, UFRGS, Porto Alegre, RS, Brazil

[c]Laboratório de Biologia Molecular de Cestódeos, Centro de Biotecnologia, UFRGS, Porto Alegre, RS, Brazil

[d]Biological Mass Spectrometry Laboratory, Clinical Chemistry Branch, Division of Laboratory Sciences, National Center for Environmental Health, Centers for Disease Control and Prevention, Atlanta, GA, United States of America

Abstract

Mesocestoides corti (syn. *vogae*) is a useful model for developmental studies of platyhelminth parasites of the Cestoda class, such as *Taenia* spp. or *Echinococcus* spp. It has been used in studies to characterize cestode strobilation, i.e. the development of larvae into adult worms. So far, little is known about the initial molecular events involved in cestode strobilation and, therefore, we carried out a study to characterize newly synthesized (NS) proteins upon strobilation induction. An approach based on bioorthogonal noncanonical amino acid tagging and mass spectrometry was used to label, isolate, identify, and quantify NS proteins in the initial steps of *M. corti* strobilation. Overall, 121 NS proteins were detected exclusively after induction of strobilation, including proteins related to development pathways, such as insulin and notch signaling. Metabolic changes that take place in the transition from the larval stage to adult worm were noted in special NS protein subsets related to developmental processes, such as focal adhesion, cell leading edge, and maintenance of location. The data shed light on mechanisms underlying early steps of cestode strobilation and enabled identification of possible developmental markers. We also

*Corresponding author at: Laboratório de Genômica Estrutural e Funcional, Centro de Biotecnologia/UFRGS, Caixa Postal, 15005 Porto Alegre, RS, Brazil. henrique@cbiot.ufrgs.br (H.B. Ferreira).

[1]Present address: Gerência Médica, Hospital Moinhos de Vento, Porto Alegre, Brazil.

[2]Present address: Serviço de Hemoterapia, Irmandade Santa Casa de Misericórdia de Porto Alegre, Porto Alegre, Brazil.

Supplementary data to this article can be found online at https://doi.org/10.1016/j.jprot.2020.103939.

Declaration of Competing Interest

Authors declare no conflicts of interest.

consider the use of developmental responsive proteins as potential drug targets for developing novel anthelmintics.

Biological significance: Larval cestodiases are life-threatening parasitic diseases that affect both man and domestic animals worldwide. Cestode parasites present complex life cycles, in which they undergo major morphological and physiological changes in the transition from one life-stage to the next. One of these transitions occurs during cestode strobilation, when the mostly undifferentiated and non-segmented larval or pre-adult form develops into a fully segmented and sexually differentiated (strobilated) adult worm. Although the proteomes of *bona fide* larvae and strobialted adults have been previously characterized for a few cestode species, little is still known about the dynamic of protein synthesis during the early steps of cestode strobilation. Now, the assessment of newly synthesized (NS) proteins within the first 48 h of strobilation the model cestode *M. corti* allowed to shed light on molecular mechanisms that are triggered by strobilation induction. The functional analyses of this repertoire of over a hundred NS proteins pointed out to changes in metabolism and activation of classical developmental signaling pathways in early strobilation. Many of the identified NS proteins may become valuable cestode developmental markers and their involvement in vital processes make them also good candidate targets for novel anthelmintic drugs.

Keywords

M. corti ; Newly synthesized proteins; Strobilation; Cestoda; Development

1. Introduction

The Cestoda class (cestodes or tapeworms) of the Platyhelminthes phylum include parasites that, especially in their larval stages, cause important diseases in humans and domestic animals. For instance, the larval (metacestode) stages of cestodes of the genus *Echinococcus* and *Taenia* cause different forms of echinococcosis and cysticercosis, respectively, which are nearly worldwide spread and very severe [1–4]. Despite their relevance for public human and animal health, these diseases are often overlooked, as evident by their inclusion in the World Health Organization's list of neglected tropical diseases [5]. These cestode larval infections can be fatal and are difficult to treat because of the relative inefficiency of available anthelmintic drugs and the emergence of parasite's drug resistance [6,7].

Cestodes are also of special interest biologically because of the ways they have evolved, developed, and adapted to parasitism. Cestodes have adapted to parasitic life in many important ways. These include asexual reproduction capabilities, the use of different host species, and the complete lack of a digestive system [8–10]. Moreover, the eucestodes (the "true" tapeworms, that belong to the Eucestoda subclass) have evolved a particularly interesting life cycle [11]. Larval forms of eucestodes undergo strobilation to produce adult worms with increased reproductive capacity, as it includes the generation of serially repeated reproductive organs (proglottization). In some eucestode species, including those of more epidemiologic relevance, proglottization is accompanied by segmentation (with the external definition of segments, called proglottids). So far, little is known about the molecular mechanisms underpinning cestode strobilation or other developmental processes.

Our current knowledge is limited to the identification of a few cell signaling pathways [12–15].

Cestode development, although of great importance for basic and applied science, is complex and poorly characterized. Furthermore, the study of cestode development is challenging from the experimental point of view. For instance, cestodes are not amenable to classic genetic approaches. Few (and not very efficient) protocols are available for transfection and RNA interference for most species [16]. Species of medical and veterinary relevance present additional difficulties because of limitations in accessing parasite material and to safety issues for the manipulation of human-infective forms [17]. Model species, such as *Mesocestoides corti* (syn. *vogae*), are helpful in the sense that they can be obtained in large amounts, easily maintained in culture, and safely manipulated [18]. Moreover, the whole *M. corti* strobilation development, from the tetrathyridium (TT) larval form to the sexually mature and fully strobilated (ST) adult worm, can be induced and followed *in vitro* [19].

The *M. corti* strobilation process is typical of cestodes. It involves evident rearrangements in body architecture, with modifications in external and internal structures [20]. Our group has assessed this process at the molecular level in previous transcriptomic and proteomic works [21–23]. Those studies, however, mostly focused on comparisons between TT forms and ST worms. Early steps of *M. corti* strobilation were only preliminarily assessed by a comparative proteomic study between *bona fide* TTs and TTs after 24 h of induction of strobilation [24]. That study was limited in scope, considering that we analyzed only steady state protein contents and used a relatively less sensitive MS instrument, which was the best technology available at that time.

A thorough understanding of molecular and cellular functions responsible for the start and initial steps of a developmental process, such as strobilation, requires a dynamic view of the proteome [25]. For that, temporal resolution is essential to describe the immediate responses of cells to environmental clues and to distinguish those from secondary or tertiary responses. A way to assess primary cell response upon development induction is by tagging and identifying newly synthesized (NS) proteins. This can be achieved by bioorthogonal noncanonical amino acid tagging (BONCAT) [26], followed by identification of tagged NS proteins by MS/MS. Such an experimental approach has been used to identify NS proteins in *Echinococcus granulosus* pre-adults (protoscoleces) when activated by pepsin treatment [27].

In the present work, we assessed the dynamics of protein synthesis in the initial steps of *M. corti* strobilation through selective labeling, purification, identification, and quantification of *M. corti* NS proteins at 24 h and 48 h after induction of strobilation. We compared NS proteins exclusively detected in the induced and tagged samples to the corresponding controls (neither induced nor tagged). This allowed us to define proteins and molecular/cellular functions triggered by induction of strobilation and involved with the early steps of *M. corti* developmental process. Some of the identified NS proteins have potential as developmental markers of cestode strobilation or as targets for the development of novel anthelmintic drugs.

2. Materials & methods

2.1. Collection and cultivation of M. corti and the metabolic incorporation of AHA

We obtained *M. corti* metacestode larvae (TTs) from experimentally infected BALB/c mice as previously described by Markoski et al. [19]. All procedures involving animals were previously approved by the Ethical Committee (Comissão de Ética no Uso de Animais, CEUA) of the Universidade Federal do Rio Grande do Sul (Project no. 32793). *In vitro* TT cultures and strobilation induction were carried out as described by Camargo de Lima et al. [21]. To label NS proteins, we incorporated the methionine analog azido-homo-alanine (AHA) into cultured TTs, essentially as described by Debarba et al. [27].

Fig. 1 shows the overall experimental design used to generate the analyzed samples. In standard cultivation conditions, TTs were cultured in RPMI 1640 medium in an atmosphere of 5% CO_2–95% N_2 at 37 °C, for up to 48 h (non-induced and non-labeled control samples). To generate the induced TTs samples, TTs were cultured in standard conditions for 24 h and then treated for induction of strobilation with trypsin (10^5 BAEE/mL) in RPMI medium supplemented with 20% fetal bovine serum (FBS) for 24 h in an atmosphere of 5% CO_2–95% N_2 at 39 °C (induced and non-labeled control samples).

To generate AHA-labeled induced samples, TTs were cultured in standard cultivation conditions for 24 h. They were then treated for induction of strobilation (as described above) in labeling condition (RPMI without methionine, Gibco, Grand Island, NY, USA; supplemented with AHA, Invitrogen, Eugene, OR, USA; to a final concentration of 50 μM) in an atmosphere of 5% CO_2–95% N_2 at 39 °C for 24 h (24 h-IND-AHA samples). Induced TTs were maintained in the labeling condition, supplemented with 10% FBS in an atmosphere of 5% CO_2–95% N_2 and 39 °C, for an additional 24 h (48 h-IND-AHA samples).

To generate AHA-labeled but not induced control samples, TTs cultivated in standard conditions for 24 h were subsequently cultured in labeling conditions supplemented with 10% FBS in an atmosphere of 5% CO_2–95% N_2 and 39 °C for an additional 24 h (24 h-NI-AHA samples) or 48 h (48 h-NI-AHA samples).

All cultures were inspected daily through an optical microscope (Zeiss Axiovert 25) for assessment of TT motility and morphology. All samples were generated in triplicates (biological replicates).

2.2. Differential interference contrast microscopy

For differential interference contrast (DIC) microscopy, TT, 24 h-IND, and 48 h-IND samples were fixed in Karnovsky solution (glutaraldehyde 2.5%, paraformaldehyde 4.0%, and cacodylate 0.1 M) for 24 h, with moderate shaking. Fixed samples were washed with phosphate-buffered saline (2 × 500 μL), stored in 0.1 M cacodylate buffer (pH 7.2), and analyzed in a Nikon Eclipse 80i microscope in diffferential interference contrast (DIC) mode. The images were acquired with the attached digital camera (Nikon DS-U3).

2.3. Mass spectrometry analysis

We used the Click-iT Protein Enrichment Kit (Invitrogen, Eugene, OR, USA), according to manufacturer's instructions, to isolate *M. corti* NS proteins. Briefly, the *M. corti* samples were incubated in urea lysis buffer (8 M urea, 200 mM Tris, pH 8.0, 4% CHAPS, 1 M NaCl) supplemented with protease inhibitors (Sigma, St. Louis, MO, USA) on ice for 10 min. The lysate was sonicated for 3 × 30 s (30% amplitude) with a 60 s interval between pulses, vortexed for 5 min, and centrifuged at 10,000 ×*g* at 4 °C for 5 min. An 800 μL aliquot of supernatant was used for Click chemistry reactions with alkyne agarose resin. Proteins were reduced with dithiothreitol at 70 °C and alkylated with iodoacetamide at room temperature. The resin was washed with 5 × 2 mL SDS wash buffer, 10 × 2 mL 8 M urea, and 10 × 2 mL 20% acetonitrile for the stringent removal of non-specifically bound proteins. The resin-bound proteins were transferred to a clean tube and digested with trypsin (10 μL of 0.1 μg/μL, Promega, Madison, WI, USA) in approximately 200 μL of digestion buffer (100 mM Tris, 2 mM $CaCl_2$, 10% acetonitrile). After a 5-min centrifugation at 1000 ×*g*, the supernatant was treated with 2% acetonitrile, acidified with trifluoroacetic acid, and desalted in HLB cartridges (Waters, Milford, MA, USA). The peptides were then eluted with 300 μL of 50% acetonitrile/0.1% TFA, quantified using a NanoDrop spectrophotometer (Thermo Fisher Scientific, Waltham, MA, USA) at 205 nm and dried in a SpeedVac concentrator (Thermo Fisher Scientific).

LC-MS/MS analyses were performed essentially as reported by Debarba et al. [27]. Briefly, peptides were reconstituted using 0.1% formic acid (Thermo Scientific, Rockford, IL, USA) in water and loaded onto a nanoAcquity UltraPerfomance liquid chromatography (LC) system (Waters Corporation, Milford, MA). Solvents A and B, 0.1% formic acid in water and 0.1% formic acid in acetonitrile (Honeywell Burdick & Jackson, Morristown, NJ, USA), respectively, were used in the mobile phase. The gradient flow was set at 300 nL/min. The gradient consisted of a hold at 5% B for 5 min, followed by a ramp up to 35% B over 25 min, then a ramp up to 95% B in 5 min, a hold at 95% B for 5 min before returning to 5% B in 5 min, and re-equilibration at 5% B for 20 min.

We used an Orbitrap Elite tandem mass spectrometer (Thermo Scientific, San Jose, CA, USA) to analyze peptides. A 2.0 kV voltage was applied to the nano-LC column. The mass spectrometer was programmed to perform data-dependent acquisition by scanning the mass range from mass-to-charge (*m/z*) 400 to 1600 at a nominal resolution setting of 60,000 for parent ion acquisition in the Orbitrap. For the MS/MS analysis, the 15 most intense ions with two or more charges were isolated and fragmented in a second round of MS.

The three biological replicates of each of the negative control samples ('non-induced and non-labeled' and 'induced and non-labeled' controls) were pooled prior to the corresponding MS analyses. Proteins identified in these negative control samples, which bound to the alkyne agarose resin despite of being unlabeled, were considered unspecific background. Biological replicates of all other samples were individually analyzed, in order to allow validation of identified proteins in each experimental time point based on their presence in at least two of the three replicates. All samples (pooled and individual) were analyzed using LC-MS/MS in triplicate runs (technical replicates).

2.4. Database search and protein identification parameters

Peak lists in the MS/MS raw data were exported in Mascot Generic Format (.mgf) using msConvert tool (version 3; ProteoWizard, Palo Alto, CA, USA) [28]. Searches in the *M. corti* protein database (deduced amino acid sequences from the *M. corti* genome assembly annotation available in the WormBase ParaSite (version WBPS9) [29] were performed using Mascot Search Engine (version 2.3.02; Matrix Science, Boston, MA, USA). The search parameters included fragment ion mass tolerance of 1 Da and peptide ion tolerance of 10 ppm. Carbamidomethylation of cysteines was specified as a fixed modification, and oxidation of methionine was specified as a variable modification.

MS/MS data were analyzed in Scaffold (version 4.4.1.1; Proteome Software Inc., Portland, OR, USA) to validate protein identifications; MASCOTdat files were loaded on Scaffold [30]. Peptide or proteins identifications were accepted if they could be established at greater than 95% or 99% of probability, as assigned by the Peptide Prophet algorithm [31] and Protein Prophet algorithm [32], respectively, and contained at least two identified peptides. The false discovery rate (FDR) (decoy), was < 1% for proteins and peptides. Scaffold was used to calculate the normalized spectral abundance factor (NSAF) [33] for each protein. Quantitative differences between NSAF values in different samples were statistically analyzed using Student's *t*-test and *p*-value correction with the Benjamini-Hochberg FDR in Perseus software (MaxQuant, version 1.5.5.1) [34]; values of $p < 0.05$ were considered statistically significant.

2.5. Functional annotation and GO term enrichment analysis

A customized search for functional annotation and gene ontology (GO) term enrichment analysis of detected proteins was performed using the Cytoscape plugin BiNGO 3.0.3 [35]. The files associated with *M. corti* protein annotation data were courteously provided by Well-come Trust Sanger Institute (UK), and the ontology files were retrieved from the GO database [36]. Functional enrichment analysis was performed using hypergeometric distribution and *p*-value correction with the Benjamini-Hochberg FDR. Values of $p \leq 0.05$ were considered statistically significant. The resulting lists of enriched GO terms were summarized by removing redundant GO terms using REVIGO [37]. The semantic similarity of the GO terms was calculated through SimRel (default allowed similarity = 0.7) and the results were plotted using R [38].

2.6. Ortholog definitions and drogability assessment

Searches for orthologs of the *M. corti* genes encoding the assessed NS proteins in initial strobilation were performed in the genomes of three representative cestode species, namely *Echinococcus multilocularis, Taenia solium*, and *Hyminolepis microstoma*. These three genomes were chosen among other whole sequenced genomes from cestode species due to their more advanced stages of assembling and annotation. Searches for ortholog proteins were carried out in the WormBase ParaSite database (version WBPS14) with the BioMart (http://www.biomart.org/) mining tool. Additional searches for orthologs were performed with the OrthoFinder software [39] using default parameters.

Druggability potential of the *M. corti* NS proteins during initial strobilation was evaluated based on available data for ortholog proteins in public databases. It was initially evaluated based on the druggability ranking of *E. multilocularis* ortholog proteins [10], and complemented by information on druggability potential and predicted best interacting molecules recovered from the TDR Targets Database (https://tdrtargets.org/) [40]. Information on the commercial availability of drugs were recovered from MolPort (https://www.molport.com/).

2.7. Assessment of RNA-seq data available for M. corti newly synthesized proteins upon strobilation induction

RNA-seq data for *M. corti* mRNA repertoires of TTs and fully ST adult worms, available at the NCBI database (Accession number SRP133301; (https://www.ncbi.nlm.nih.gov/sra/SRP133301) have been previously processed and assembled to generate the corresponding transcriptome assemblies [22]. To allow comparisons between *M. corti* transcriptomic and proteomic expression data, gene IDs used for RNA-seq data analyses [16] were compatibilized with the gene IDs of the *M. corti* genome assembly version 1.0.4 (Accession number PRJEB510), available at the WormBase ParaSite version WBPS13 (ftp://ftp.ebi.ac.uk/pub/databases/wormbase/parasite/releases/WBPS13/species/mesocestoides_corti/PRJEB510/), by direct sequence alignments. Differential expression between *bona fide* TTs and adult worms was established for NS protein-encoding genes based on their RNA-seq fragments per kilobase million (FPKM) expression values in each developmental stage. To measure possible linear correlation between protein NSAF values and mRNA FPKM values, Pearson's correlation coefficients and *p*-values were calculated using Microsoft Excel and the *P* Value from Pearson (R) Calculator tool from Social Science Statistics (https://www.socscistatistics.com/pvalues/pearsondistribution.aspx). For some of the performed analyses, NS protein-encoding genes were ordered based on their FPKM values (from the lowest to the highest one) in TTs and divided into a group of genes with lower (below the average) expression and a group with higher (above the average) expression.

3. Results and discussion

3.1. Identification of M. corti NS proteins upon strobilation induction

Cestode strobilation is a complex developmental process, that involves evident rearrangements in body architecture, with modifications in both external and internal structures [20]. *M. corti* has been chosen as a model organism in this work and in previous studies addressing cestode strobilation [41–44] because it allows to induce and follow, in controlled culture conditions, the whole developmental process from the TT larval form to the fully ST adult worm [45]. In previously optimized *M. corti in vitro* conditions [19], essential requirements naturally found in definitive hosts, are sufficiently provided by controlled temperature and atmospheric conditions, induction by protease treatment, and culture in serum-rich medium. *In vitro*, TTs are then able to develop and undergo a typical cestode strobilation development, producing mature, sexually-differentiated proglottids without the generation of aberrant forms.

In our experimental conditions, *M. corti* strobilation efficiency was > 90%. Visual inspection by optical microscopy of cultured TTs showed the expected elongation of the specimens in induced samples in comparison to those kept in standard conditions (without induction). To further characterize the morphology of the initial steps of *M. corti* strobilation studied in this work, parasites were followed using DIC microscopy up to 48 h after induction of strobilation (Fig. 2). Typically, non-induced control TTs (Fig. 2A) averaged 750 μm in length, with evident suckers and a thin constriction below the suckers. Some changes in length and morphology were observed after induction of strobilation (Fig. 2A *vs.* B and C). After 24 h of induction (Fig. 2B), TTs were typically 850 μm long and showed a clear constriction below the suckers, corresponding to the neck region that delimits the scolex from the strobilum. After 48 h, the worm was elongated (up to 2.5 mm long), with a clearer separation of the head (scolex) region (with the suckers) from the yet non-segmented strobilar region (Fig. 2C). The observed developmental behavior was in line with previous studies, that showed that neck formation is an early strobilation event [46]. The intensive cell proliferation that occurs in this region [47] results in strobilum elongation. We chose the 48 h timeframe to assess, at the molecular level, the early strobilation steps that precede the later ones, which eventually give rise to segmentation and proglottid formation [46]. This early strobilation timeframe was chosen because previous proteomic and transcriptomic studies have mostly addressed the starting and ending points of *M. corti* strobilar development, *i.e.* the *bona fide* TT and/or the fully ST adult worm [21,22,48–51].

Here, *M. corti* early steps of strobilation were assessed at the molecular level using a proteomic approach based on BONCAT for the selective labeling of NS proteins with AHA. In our proteomic experimental design, proteins synthesized by *M. corti* for 24 h and 48 h after strobilation induction were specifically labeled by BONCAT, captured onto an alkyne resin *via* Click chemistry, and identified using LC-MS/MS. The BONCAT-labeling of NS proteins has been used to study various model organisms, from bacteria to vertebrates and plants [52–56]. Our group also used it for studies on the cestode parasite *E. granulosus* [27]. In all these previous studies with the BONCAT system, the AHA labeling reagent was non-toxic and did not alter the global protein synthesis rates or caused detectable protein misfolding or degradation. Indeed, no motility or morphological differences were observed between AHA labeled and unlabeled *M. corti* samples (data not shown).

In order to assure confidence and reproducibility of our proteomic data, only proteins with at least two peptides and present in at least two of the three biological replicates of each sample were considered for protein identification. Proteins detected in the non-induced and non-labeled control samples and in induced and non-labeled control samples were removed from the analyses. The remaining proteins recovered from each AHA-labeled test sample were assumed to be newly synthesized (NS proteins). Table S1 shows the full list of detected peptides from all samples. Table S2 list the identified proteins.

Fig. 3 shows the overall numbers of LC-MS/MS-identified NS proteins. Overall, 186 *M. corti* unique proteins were detected after 24 h of *in vitro* cultivation, including 166 proteins from 24 h-IND-AHA samples and 98 from 24 h-NI-AHA samples (Fig. 3A and Table S2A and B). A total of 78 proteins (41.9%) were shared between 24 h-IND-AHA and 24 h-NI-AHA samples. Moreover, 88 (47.3%) and 20 (10.8%) were exclusively detected in the

24 h-IND-AHA and 24 h-NI-AHA samples, respectively. After 48 h of *in vitro* cultivation, 182 unique proteins were detected, including 172 proteins in 48 h-IND-AHA samples and 100 proteins in 48 h-NI-AHA samples (Fig. 3B, and Table S2 C–D). A total of 90 proteins (49.5%) were shared between 48 h-IND-AHA and 48 h-NI-AHA samples. Other 82 (48.1%) and 10 (5.5%) proteins were exclusively detected in the 24 h-IND-AHA and 24 h-NI-AHA samples, respectively.

It is also important to highlight that, among the overall repertoire of *M. corti* proteins newly synthesized upon induction of strobilation (121 unique proteins), there were 19 proteins of unknown function (UF proteins), corresponding to genes annotated in public databases as hypothetical ones. The detection of the corresponding protein products of these formerly hypothetical genes confirmed them as functional protein coding genes. Such contribution of ours and others' proteomic surveys is relevant for the improvement of genome annotations, as the advancements in genome sequencing have led to a rapidly growing list of putative genes (predicted coding DNA sequences), that depend on the identification of their expression products for functionality confirmation [57].

3.2. Definition of the M. corti sets of early, early persistent, and late NS proteins

For assessing the dynamics of protein synthesis during initial steps of *M. corti* strobilation (post induction), only the set of 170 NS proteins exclusively detected in 24 h-IND-AHA (88 proteins) or 48 h-IND-AHA (82 proteins) were considered (Fig. 3C). These NS proteins (Tables 1–3) were classified into three groups, based on the temporal window of their detection along the timeframe assessed in the experiments. NS proteins detected only in 24 h-IND-AHA samples (39 proteins, 32,2%) were assigned as early proteins (Table 1); proteins detected in both the 24 h-IND-AHA and 48 h-IND-AHA samples (49 proteins, 40.5%) were assigned early persistent proteins (Table 2); and, finally, NS proteins detected only in 48 h-IND-AHA (33 proteins, 27.3%) were assigned late proteins (Table 3).

Overall, these three defined datasets comprehended proteins whose syntheses were triggered or enhanced by inducing stimulae in initial strobilation. They represent a significant incremental advance in relation to the few proteomic studies that have been carried so far focusing in cestode strobilation. Our group recently assessed the TT proteome, but in comparison to that of fully ST adult worms [21]. The first 24 h of cestode strobilation was also previously assessed in *M. corti*, in a pioneer proteomic study [24], and in *E. granulosus*, in a survey of NS proteins in pepsin-treated (activated) protoscoleces [27]. In comparison to these previous studies, the present work provided significant incremental advances, by addressing NS proteins using state-of-the art experimental approaches for protein labeling and identification, and by adding in our experimental design a second time point at 48 h after induction of strobilation. As far as we are aware of, the provided developmental timeframe between 24 h and 48 h of cestode strobilation is here being assessed for the first time using an 'omics' approach.

The group of early NS proteins (Table 1) included those whose expression was activated in the first 24 h of the strobilation process but did not persist longer. Among them, it was noticeable the presence of some proteins related to signal transduction, including two importins (importin subunit alpha and putative importin 7), an ankyrin repeat-containing

domain-containing protein, and protein kinase-like domain containing protein; and some associated with cellular differentiation (*e.g.*, acidic leucine-rich nuclear phosphoprotein 32 family member A, hepatocyte growth factor-regulated tyrosine kinase substrate, and epsin-like N-terminal domain containing protein). Importins, as components of the insulin signaling pathway [58], and epsin-like protein, a component of the notch signaling pathway [59], have all been implicated in developmental processes, including in cestodes [60]. Therefore, their presence as NS proteins in 24 h-IND-AHA samples suggests the activation of these two signaling transduction pathways as an initial response to the strobilating stimulant in *M. corti*. Ankyrin-like and kinase-like proteins also have been implicated in signal transduction [61,62], providing evidence of the involvement of additional cell signaling events in early strobilation of this parasite.

Among the early group of NS proteins there were also many related to protein synthesis, including the eukaryotic translation initiation factor 5B (eIF5B), 40S ribosomal protein SA, 60S acidic ribosomal protein P0, 40S ribosomal protein S3, 40S ribosomal protein SA, and 60S acidic ribosomal protein P0. The translational GTPase eIF5B catalyzes the joining of the 40S and 60S ribosomal subunits [63], and its upregulation supports general translation in cells known to have reduced protein synthesis, such as *Xenopus laevis* oocytes and mouse embryonic stem cells [64]. In such cells, this protein plays a role in regulating specific developmental stages and cell state transitions [64]. In *M. corti*, the detected expression of eIF5B expression and other translation-related proteins in 24 h-IND-AHA samples could indicate a protein synthesis boost as an early step in the strobilation process. Moreover, other early NS proteins provided evidences of the enhancement of protein turnover (*e.g.*, 26S protease regulatory subunit 8, 26S proteasome non-ATPase regulatory subunit 7, and trypsin-like cysteine/serine peptidase domain-containing protein) and transport systems (*e.g.*, kinesin heavy chain, kinesin light chain 3, DLI-1, and two isoforms of dynein light chain, and type 1/2 family-containing protein).

The group of early persistent NS proteins (Table 2) comprehended those whose expression started early upon strobilation activation and persist being synthesized for at least 48 h. Interestingly, this group included some proteins involved with gene/protein expression, as the transcription factor BTF3, the suppressor of presenilin-2 (SRP-2), the eukaryotic initiation factor 4A (eIF4F), and the elongation factor Tu mitochondrial; as well some involved with cell signaling (*e.g.*, adenylate kinase isoenzyme 1, serine/threonine protein-kinase MAX-2, and nucleoside diphosphate kinase); and protein modification (prolyl endopeptidase, and trypsin-like cysteine/serine peptidase domain-containing protein). Also in this group there was a set of structural proteins, as protein PLST-1, adducin related protein 1, tubulin beta-2 chain and peroxidasin (PXN), that may be involved in cytoskeleton rearrangements during cell differentiation. Overall, these early persistant proteins are suggestive of initial and persistent activation of developmental gene/protein expression programs responsible for the strobilation steps that occur within 48 h after induction of strobilation. In line with that, SRP-2, eIF4F and PXN have been associated with important roles in the development of model organisms, such as *Caenorhabditis elegans*, *Drosophila melanogaster*, and *Mus musculus* [65–67].

Finally, the group of late NS proteins (Table 3) included those whose synthesis started between 24 h and 48 h after strobilation induction. In this group there were some involved with cell signaling, including two protein phosphatases (serine/threonine-protein phosphatase PP2A 65 kDa regulatory subunit, and probable protein phosphatase 2C), guanine nucleotide-binding protein subunit beta-1, adducin-related protein 1, and a PDZ domain-containing protein. Among the late proteins there were also some related to cell organization (coronin, and cell polarity protein), to vesicle trafficking (charged multivesicular body protein 3, endophilin-A, and calnexin), and to proteolytic processing in organelles (a lysosomal saposin-related protein, and mitochondrial-processing peptidase subunit beta).

Several NS proteins of this late group have had their orthologs studied in other species and implicated in cellular and developmental process that can be easily envisioned as part of cestode strobilation processes. For instance, signal transducing proteins, like protein phosphatases and their kinase counterparts, are known to play roles in the regulation of some important cellular processes, including development-related ones [68–70], while PDZ domain-containing proteins have been shown to be central to organizing diverse cell signaling assemblies [71,72]. Coronin and endophilin-A, in turn, have been both associated with nervous system development and function. In *C. elegans*, coronin is expressed in neuroblasts, and is required for larval neural development [73], and in *D. melanogaster*, endophilin A is expressed specifically in the central nervous system and is essential for synaptic vesicle endocytosis [74]. Moreover, cell polarity proteins are conserved throughout evolution and, by reacting to extrinsic or intrinsic polarity cues, are crucial for developmental cell polarization events [75]. Overall, these proteins and functions would represent the later step of initial strobilation step, corresponding to a transition between the initial developmentally activated strobilating state to a progressively more elongated and differentiated state.

As proteins may undergo cycles of expression during development, we also surveyed available proteomic data for *M. corti* adult worms [21] to verify whether any of the 121 NS proteins identified in initial steps of strobilation were also detected by the end of this process. From the 39 proteins in the early group, only one was also found in adults, and, from the 82 proteins being synthesized at the 48 h time point (i.e, the sum of those NS proteins in the the early persistent group and those in the late group), 12 were detected adult worms (Table S3). The detection of these proteins in adult worms points out to their relevance also in later steps of the strobilation process. The full dynamics of expression of these proteins remains to be investigated, and, upon a better characterization of their temporal dynamics of expression, some of them may become useful marks of developmental time points.

It is also important to notice that, among the overall repertoire of *M. corti* 121 NS proteins in the initial steps of strobilation, there were 5 UF proteins, corresponding to genes formerly annotated in public databases as hypothetical ones. Three UF proteins were identified in the early persistent group and two, in the late group. Moreover, four of the UF proteins were found exclusively among flatworm species, and one was also associated with cestode strobilation, based on *in silico* comparative genomic and transcriptomic analyses recently

carried out by our group [76]. Based on these evidences, these UF proteins will deserve further studies to assess their possible roles in cestode-specific developmental mechanisms.

3.3. Functional enrichment analysis of NS proteins in initial steps of M. corti strobilation

To identify molecular functions that became enriched upon *M. corti* induction of strobilation, functional enrichment analyses were performed for the whole sets of NS proteins detected in 24 h-IND-AHA samples (166 proteins) and 48 h-IND-AHA samples (172 proteins). These GO functional enrichment analyses allowed us to categorize a total of 148 (89%) proteins in 24 h-IND-AHA samples (Table S4A), and 149 proteins (86%) in 48 h-IND-AHA samples (Table S4B), according to biological process, molecular function, and cellular component GO terms. No GO term assignments were obtained for 18 proteins in 24 h-IND-AHA samples, and for 23 proteins in 48 h-IND-AHA samples. The GO terms assigned to NS proteins from 24 h-IND-AHA samples and 48 h-IND-AHA samples were summarized using REVIGO (Figs. 4A–B, Tables S5A–C).

The 24 h-IND-AHA samples were exclusively enriched in 14 GO terms (Table S5C), that mostly corresponded to cell structure and metabolism. In this set of enriched GO terms, there were 6 representing basic metabolic functions (including, ‘carboxylic acid metabolic process’, ‘GTPase activity’, and ‘pyrophosphatase activity’), and other 6 related to cell organization (*e.g.* ‘microtubule based process’, ‘cellular component organization’, and ‘organelle part’). Overall, these enriched GO terms are suggestive of intense cell structural rearrangements and metabolic activities, including generation of precursor metabolites and energy, within the first 24 h after strobilation induction.

A total of 29 GO terms were enriched only in 48 h-IND-AHA samples (Table S5C). They included at least 13 related to basic metabolic processes (including ‘carbohydrate metabolic process’, ‘glucose 6-phosphate metabolic process’, ‘pyruvate dehydrogenase activity’, and ‘thioester metabolic process’), 3 related to purine and/or pyrimidine nucleotide metabolism (‘nucleoside diphosphate metabolic process’, ‘purine-nucleoside phosphorylase activity’, and pyridine-containing compound metabolic process), and at least 6 related to cell structure or differentiation (*e.g.* ‘focal adhesion’, ‘cell leading edge’, ‘maintenance of location’ and ‘organelle organization’). Taken together, these enriched GO terms reinforce the idea of an overall increase in metabolic activities during the early steps of strobilation, with fuel mobilization and energy production. They also point out to functions related to the metabolism of nucleic acid precursors, and, as such, implicated in RNA transcription and DNA replication, as well to other functions indicative of cellular proliferation and differentiation.

A still more comprehensive picture of the functional processes operating during the early steps of strobilization may be inferred from the set of 70 GO terms that were enriched in both 24 h-IND-AHA and 48 h-IND-AHA samples (Table S5C). This shared set included many enriched GO terms related to basic metabolism and energy production (*e.g.*, ‘metabolic process’, ‘small molecule metabolic process’; ‘cellular carbohydrate metabolic process’, ‘organic acid metabolic process’, ‘generation of precursor metabolites and energy’, and ‘energy derivation by oxidation of organic compounds’); along with others related to RNA and/or DNA synthesis (*e.g.* ‘nucleobase-containing small molecule metabolic process’,

'purine-containing compound metabolic process', 'nucleotide phosphorylation', and 'purine ribonucleoside triphosphate metabolic process') and protein synthesis (*e.g.* 'translational elongation', 'translation elongation factor activity', and 'unfolded protein binding'); cell structure and differentiation (*e.g.*, cellular component organization or biogenesis, 'cytoskeleton organization', 'structural constituent of cytoskeleton', and 'contractile fiber part'); and developmental processes (*e.g.* 'developmental process', 'cellular process involved in reproduction', and 'single-organism developmental process'). Overall, these GO terms enriched in the first 48 h of *M. corti* strobilation depict a transition scenario, from the relatively quiescent larval TT stage, to a growing, differentiating and metabolically more active strobilating worm.

3.4. Evolutive conservation and druggability of NS proteins in initial steps of M. corti strobilation

The *M. corti* genome (NCBI accession number PRJEB510) has 10,589 protein coding genes, around 70% of which have identifiable orthologs in the genomes of other cestode species "(Paludo GP, personal communication)". Interestingly, virtually all the 121 unique *M. corti* proteins here identified as NS in initial strobilation steps had orthologs identified in a comparative analysis performed with other three representative cestode species, *E. multilocularis*, *T. solium*, and *H. microstoma* (Table S6), with the exceptions of a hypothetical protein (MCOS_0000288501), in *E. multilocularis*, *T. solium*, and *H. microstoma*. This points out to an overall conservation of proteins involved in the initial strobilation events among *M. corti* and other cestodes, including species from genera of medical and/or veterinary importance, like *Echinococcus*, *Taenia*, and *Hymenolepis*. Moreover, the degrees of conservation between the *M. corti* NS proteins with their orthologs of these cestodes species are relatively high, with average identities of > 74% (Table S6). Such conservation is important, considering that many of the *M. corti* NS proteins in initial strobilation steps may be essential for parasite survival and development, and, as such, at least some of them can be regarded as potential targets for drug development.

Considering that novel and more efficient anthelmintics are necessary, especially for the treatment of chronic visceral cestodiases, like echinococcoses and cysticercoses [1], a preliminary assessment of the potential druggability of the NS proteins identified upon strobilation induction was carried out based on the available data for their *E. multilocularis* orthologs [10]. From the 121 *M. corti* NS proteins, 120 had orthologs in *E. multilocularis*, whose druggability ranked from 13 to 5443 (Table S7). As top-ranked proteins based on their druggability scores may be considered more druggable than the lower ranked ones [10,77], it is important to emphasize that 9 of the *M. corti* NS proteins had orthologs among the top-100 druggable proteins in *E. multilocularis*, namely aldo-keto reductase family 1 member C-like protein 1; putative aspartyl-tRNA synthetase; JYalpha (*M. corti* paralog 1); JYalpha (*M. corti* paralog 2); P-type ATPase, A domain-containing protein; cysteinetRNA ligase, cytoplasmic; NAD(P)-binding domain-containing protein; UDP-glucose 4-epimerase; and serine/threonine-protein phosphatase PP2A 65 kDa regulatory subunit.

Additional searches made for the 121 *M. corti* NS proteins in the TDR Targets Database [40], a well-known data repository for the rapid identification and prioritization of molecular

targets for drug development, showed that there are predicted interacting molecules for 32 of them, and 6 of these molecules are commercially available according to the MolProt database (Table S7). Interestingly, from the six *M. corti* NS proteins potentially interacting with commercially available drugs, two (NAD(P)-binding domain-containing protein, and UDP-glucose 4-epimerase) have orthologs among the *E. multilocularis* top-100 druggable proteins, and had predicted interactions with the same commercial molecule. The use of this single commercial drug as a potential anthelmintic with effect on two well-ranked parasite protein targets is promising and deserves future evaluation.

Moreover, the International Helminth Genomes Consortium recently performed a broad comparative study of 81 genomes of parasitic and non-parasitic worms and proposed a set of high priority targets for drug development [57]. Three of these protein targets (tubulin beta-2 chain, glutathione S-transferase, and serine/threonine-protein phosphatase PP2A 65 kDa regulatory subunit) were detected as NS proteins associated with cestode strobilation in our study, reinforcing their potential as novel therapeutic targets for cestodiases and other helminthiases.

3.5. Expression regulation of NS proteins in initial steps of M. corti strobilation

So far, there have been no studies investigating how the genes encoding these proteins that are newly synthesized within the first 24 h or 48 h of strobilation are regulated. Therefore, as a first step towards the elucidation of regulatory mechanisms controlling the expression of these genes, we carried out a survey based on previously generated *M. corti* RNA-seq data [48]. This showed that all the 121 different *M. corti* proteins here identified as NS in early strobilation had their corresponding genes transcribed in TTs (Table S8). Moreover, 46 of them (38%) were differentially transcribed between TTs and fully ST adult worms, and this proportion was roughly mantained (between 35.9% and 39.4%) when this analysis was separately performed with the genes corresponding to the subsets of early, early persistent, and late NS proteins (Fig. S2). Moreover, among these 46 differentially expressed genes, 25 (54.3%) were upregulated and 21 (45.7%) were downregulated in adult worms in comparison to TTs. Overall, these observations are indicative of transcriptional regulatory mechanisms (both positive and negative) operating during strobilation for these genes, and provide further evidence of the involvement of their encoded proteins in both initial and concluding steps of this cestode developmental process.

We next assessed whether there was any correlation between NS protein abundances in initial strobilation and the transcriptional level of the corresponding genes in *bona fide* (not induced) TTs. For that, we compared the NSAF values of the NS proteins with the previously available FPKM values of their cognate genes in TTs [22] (Table S9). As shown in Table S9A, a poor, not statistically significant ($p > 0.01$) correlation, with r^2 of 0.1417, was found for the whole set of 121 NS proteins. We also performed the same correlation analysis in separate for the three groups of NS proteins, and virtually no (and also not statistically significant, with $p > 0.01$) correlation was found either for early (Table S9B) or late (Table S9D) proteins, with calculated r^2 values of 0.0047 and 0.0327, respectively. However, for the early persistent group (Table S9C), a fair, statistically significant ($p < 0.01$) correlation, with r^2 of 0.4200 was found. Therefore, these results indicate that the

gene transcriptional levels in TTs have at most a fair influence in the abundance of the corresponding NS proteins in initial strobilation, with a stronger influence in the group of the early persistent ones. This overall limited correlation between mRNA levels in TTs and NS protein levels in initial strobilation was not surprising, taking into account the well-known influence of regulatory mechanism acting at the post-transcriptional level [78–80] as well the regulatory mechanisms of gene expression likely triggered upon strobilation induction.

We further explored the available RNA-seq data to investigate whether the transcriptional levels of genes in *bona fide* TTs would be related to the timing of detection of the corresponding NS proteins after strobilation induction. Although there was only a weak to moderate correlation between TT mRNA levels and NS protein levels in initial strobilation, as shown above, it was worth it to investigate the hypothesis that the amount of mRNAs transcribed in TTs could contribute, at least in part, to define the initial pattern (timing) of synthesis de novo of the corresponding proteins upon strobilation induction. Assuming mRNA synthesis and accumulation in the TT stage as a main determinant of *de novo* protein synthesis in initial strobilation, it would be expected that early NS proteins (synthesized within the first 24 h of strobilation) would mostly correspond to genes more highly transcribed in TTs. Conversely, the late NS proteins (expressed between 24 h and 48 h after strobilation induction) would mostly correspond to genes less transcribed in TTs. To be synthesized *de novo*, these late NS proteins would require further activation or transcript accumulation of the corresponding genes after strobilation induction. To preliminarily address this issue, the whole set of genes encoding the 121 NS proteins were ordered according to their FPKM expression values, that ranged from 14.6974 to 2088.2300, with an average of 314.8158 (Table S8). The genes were then divided into two categories, one of lower (below the average) expression, which included 91 genes (75.2%), and another of higher (above the average) expression, which included 30 genes (24.8%). Next, we analyzed the distribution of the sorted genes in relation to their correspondent products in the early, early persistent and late sets of NS proteins (Fig. S1). Interestingly, the genes of lower or higher expression in TTs were distributed in quite similar proportions among the three sets of encoded NS proteins (early, early persistent, and late), with the less expressed representing from 71.4% to 81.8% and the more expressed representing 18.2 to 28.6%. Therefore, no evident tendencies of association were observed between gene transcriptional levels in TTs (*i.e.* prior to strobilation induction) and the timing of *de novo* synthesis of the encoded NS proteins in initial strobilation (at 24 h, 24 h–48 h or 48 h after strobilation induction).

Overall, the performed comparative analyses between the *de novo* synthesis and abundance of proteins in initial strobilation and the mRNA levels of their encoding genes in TTs prior to strobilation induction is suggestive of a scenario in which different mRNA half-lives and post transcriptional regulation (in processing and/or translation) can be major determinants of both the abundance and the timing of appearance of key proteins in initial strobilation. Future joint analyses of transcriptomic and proteomic data from samples of strobilating worms in different time points will be necessary to provide more insights on the various levels of gene expression regulation that may be operating. Finally, it will be important to characterize not only the temporal, but also the spatial patterns of distribution of proteins

that are differentially expressed along *M. corti* strobilation. Many of them may be associated to specific cell types, morphological structures and/or developmental events, and, as such, may become valuable markers of cestode development [18].

4. Conclusions

We assessed continuous protein synthesis during the initial steps of *M. corti* strobilation using BONCAT and mass spectrometry (LC-MS/MS). We determined the dynamics of protein synthesis through selective labeling, purification, identification, and quantification of *M. corti* NS proteins in two time points after induction of strobilation (24 h and 48 h). We identified proteins whose synthesis was triggered or enhanced by strobilation-inducing stimulae. Signaling and regulating proteins detected in developmental steps suggested that different cellular developmental pathways are activated in the initial steps of the strobilation process. We also point to metabolic changes that take place in the transition from the larval stage to adult worm. The developmental-responsive proteins identified provide several candidate molecular markers of these key *M. corti* developmental events. Some of the detected proteins also might be targets for development of novel anthelminthic drugs. The possible functions of UF proteins need further study.

Supplementary Material

Refer to Web version on PubMed Central for supplementary material.

Acknowledgments

We thank Prof. Eduardo Torres, Dr. Makoto Enoki and Msc. Ludmila Rocha, from the Universidade do Estado do Rio de Janeiro (UERJ, DMIP-FCM), for the technical support in preparing the samples for microscopy. This work was supported by Coordenação de Aperfeiçoamento de Pessoal de Nível Superior (CAPES), Conselho Nacional de Desenvolvimento Científico e Tecnológico (CNPq, Grant nr. 303287/2017–9), and by a Burroughs-Wellcome Fund Collaborative Research Travel Award, funded by the Burroughs-Wellcome Fund (USA). JCL is recipient of a CAPES Ph.D. fellowship. JAD was a recipient of a CNPq Ph.D. fellowship.

References

[1]. Wen H, Vuitton L, Tuxun T, Li J, Vuitton DA, Zhang W, et al. , Echinococcosis: advances in the 21st century, Clin. Microbiol. Rev. 32 (2019) 1–39, 10.1128/CMR.00075-18.

[2]. Kern P, Menezes da Silva A, Akhan O, Müllhaupt B, Vizcaychipi KA, Budke C, et al. , The Echinococcoses: Diagnosis, Clinical Management and Burden of Disease, Adv. Parasitol. 96 (2017) 259–369, 10.1016/bs.apar.2016.09.006. [PubMed: 28212790]

[3]. Moazeni M, Khamesipour F, Anyona DN, Dida GO, Epidemiology of taeniosis, cysticercosis and trichinellosis in Iran: a systematic review, Zoonoses Public Health 66 (2019) 140–154, 10.1111/zph.12547. [PubMed: 30575317]

[4]. Tellez-Zenteno JF, Hernandez-Ronquillo L, Epidemiology of neurocysticercosis and epilepsy, is everything described? Epilepsy Behav. 76 (2017) 146–150, 10.1016/j.yebeh.2017.01.030. [PubMed: 28526213]

[5]. Mitra AK, Mawson AR, Neglected tropical diseases: epidemiology and global burden, Trop. Med. Infect. Dis. 2 (2017) 36, 10.3390/tropicalmed2030036. [PubMed: 30270893]

[6]. De Rycker M, Baragaña B, Duce SL, Gilbert IH, Challenges and recent progress in drug discovery for tropical diseases, Nature 559 (2018) 498–506, 10.1038/s41586-018-0327-4. [PubMed: 30046073]

[7]. Idris OA, Wintola OA, Afolayan AJ, Helminthiases; prevalence, transmission, host-parasite interactions, resistance to common synthetic drugs and treatment, Heliyon 5 (2019) e01161, , 10.1016/j.heliyon.2019.e01161.

[8]. Couso JP, Segmentation, metamerism and the Cambrian explosion, Int. J. Dev. Biol. 53 (2009) 1305–1316, 10.1387/ijdb.072425jc. [PubMed: 19247939]

[9]. Zarowiecki M, Berriman M, What helminth genomes have taught us about parasite evolution, Parasitology 142 (2015) S85–S97, 10.1017/S0031182014001449 Suppl. [PubMed: 25482650]

[10]. Tsai IJ, Zarowiecki M, Holroyd N, Garciarrubio A, Sanchez-Flores A, Brooks KL, et al. , The genomes of four tapeworm species reveal adaptations to parasitism, Nature 496 (2013) 57–63, 10.1038/nature12031. [PubMed: 23485966]

[11]. Olson PD, Littlewood DTJ, Bray R a J Mariaux, Interrelationships and evolution of the tapeworms (Platyhelminthes: Cestoda), Mol. Phylogenet. Evol. 19 (2001) 443–467, 10.1006/mpev.2001.0930. [PubMed: 11399152]

[12]. Montagne J, Preza M, Castillo E, Brehm K, Koziol U, Divergent Axin and GSK-3 paralogs in the beta-catenin destruction complexes of tapeworms, Dev. Genes Evol. 1 (2019), 10.1007/s00427-019-00632-w.

[13]. Olson PD, Zarowiecki M, James K, Baillie A, Bartl G, Burchell P, et al. , Genomewide transcriptome profiling and spatial expression analyses identify signals and switches of development in tapeworms, Evodevo 9 (2018) 1–29, 10.1186/s13227-018-0110-5. [PubMed: 29387332]

[14]. Zhang S, Comparative Transcriptomic analysis of the larval and adult stages of *Taenia pisiformis*, Genes (Basel) 10 (2019) 507, 10.3390/genes10070507. [PubMed: 31277509]

[15]. Sulima A, Savijoki K, Bień J, Näreaho A, Sałamatin R, Conn DB, et al. , Comparative proteomic analysis of *Hymenolepis diminuta* cysticercoid and adult stages, Front. Microbiol. 8 (2018) 1–14, 10.3389/fmicb.2017.02672.

[16]. Spiliotis M, Mizukami C, Oku Y, Kiss F, Brehm K, Gottstein B, *Echinococcus multilocularis* primary cells: improved isolation, small-scale cultivation and RNA interference, Mol. Biochem. Parasitol. 174 (2010) 83–87, 10.1016/j.molbiopara.2010.07.001. [PubMed: 20637246]

[17]. Siles-Lucas M, Hemphill A, Cestode parasites: application of in vivo and in vitro models for studies on the host-parasite relationship, Adv. Parasitol. 51 (2002) 133–230, 10.1016/S0065-308X(02)51005-8. [PubMed: 12238890]

[18]. Koziol U, Evolutionary developmental biology (evo-devo) of cestodes, Exp. Parasitol. 180 (2017) 84–100, 10.1016/j.exppara.2016.12.004. [PubMed: 27939766]

[19]. Markoski MM, Bizarro CV, Farias S, Espinoza I, Galanti N, Zaha A, et al. , In vitro segmentation induction of *Mesocestoides corti* (Cestoda) tetrathyridia, J. Parasitol. 89 (2003) 27–34, 10.1645/0022-3395(2003)089[0027,IVSIOM]2.0.CO;2. [PubMed: 12659299]

[20]. Camargo de Lima J, Caracciolo MEME, Lima LRLR, Lopes-Torres EJEJ, Ferreira HBHB, Morphological and ultrastructural features of *Mesocestoides corti* during in vitro differentiation from larva to adult worm, Clin. Microbiol. Infect.(2019), 10.1016/j.cmi.2019.10.005.

[21]. Camargo de Lima J, Monteiro KM, Basika Cabrera TN, Paludo GP, Moura H, Barr JR, et al. , Comparative proteomics of the larval and adult stages of the model cestode parasite *Mesocestoides corti*, J. Proteome 175 (2018) 127–135, 10.1016/j.jprot.2017.12.022.

[22]. Basika T, Paludo GP, Araujo FM, Salim AC, Pais F, Maldonado L, et al. , Transcriptomic profile of two developmental stages of the cestode parasite *Mesocestoides corti*, Mol. Biochem. Parasitol. (2019) 35–46, 10.1016/j.molbiopara.2019.02.006 (Under rev. [PubMed: 30797776]

[23]. Bizarro CV, Bengtson MH, Ricachenevsky FK, Zaha A, Sogayar MC, Ferreira HB, Differentially expressed sequences from a cestode parasite reveals conserved developmental genes in platyhelminthes, Mol. Biochem. Parasitol. 144 (2005) 114–118, 10.1016/j.molbiopara.2005.07.002. [PubMed: 16139903]

[24]. Laschuk A, Monteiro KM, Vidal NM, Pinto PM, Duran R, Cerveñanski C, et al. , Proteomic survey of the cestode *Mesocestoides corti* during the first 24 hours of strobilar development, Parasitol. Res. 108 (2011) 645–656, 10.1007/s00436-010-2109-2. [PubMed: 20953630]

[25]. Veraksa A, Regulation of developmental processes: insights from mass spectrometry-based proteomics, Wiley Interdiscip. Rev. Dev. Biol. 2 (2013) 723–734, 10.1002/wdev.102. [PubMed: 24014456]

[26]. Dieterich DC, Link AJ, Graumann J, Tirrell DA, Schuman EM, Selective identification of newly synthesized proteins in mammalian cells using bioorthogonal noncanonical amino acid tagging (BONCAT), Proc. Natl. Acad. Sci. 103 (2006) 9482–9487, 10.1073/pnas.0601637103. [PubMed: 16769897]

[27]. Debarba JA, Monteiro KM, Moura H, Barr JR, Ferreira HB, Zaha A, Identification of newly synthesized Proteins by *Echinococcus granulosus* Protoscoleces upon induction of strobilation, PLoS Negl. Trop. Dis. 9 (2015) e0004085, , 10.1371/journal.pntd.0004085.

[28]. Chambers MC, Maclean B, Burke R, Amodei D, Ruderman DL, Neumann S, et al. , A cross-platform toolkit for mass spectrometry and proteomics, Nat. Biotechnol. 30 (2012) 918–920, 10.1038/nbt.2377. [PubMed: 23051804]

[29]. Howe KL, Bolt BJ, Shafie M, Kersey P, Berriman M, WormBase ParaSite − a comprehensive resource for helminth genomics, Mol. Biochem. Parasitol. 215 (2017) 2–10, 10.1016/j.molbiopara.2016.11.005. [PubMed: 27899279]

[30]. Washburn MP, Wolters D, Yates JR, Large-scale analysis of the yeast proteome by multidimensional protein identification technology, Nat. Biotechnol. 19 (2001) 242–247, 10.1038/85686. [PubMed: 11231557]

[31]. Keller A, Nesvizhskii AI, Kolker E, Aebersold R, Empirical statistical model to estimate the accuracy of peptide identifications made by MS/MS and database search, Anal. Chem. 74 (2002) 5383–5392, 10.1021/ac025747h. [PubMed: 12403597]

[32]. Nesvizhskii AI, Keller A, Kolker E, Aebersold R, A statistical model for identifying proteins by tandem mass spectrometry, Anal. Chem. 75 (2003) 4646–4658, 10.1021/ac0341261. [PubMed: 14632076]

[33]. Zybailov B, Mosley AL, Sardiu ME, Coleman MK, Florens L, Washburn MP, Statistical analysis of membrane proteome expression changes in *Saccharomyces c erevisiae*, J. Proteome Res. 5 (2006) 2339–2347, 10.1021/pr060161n. [PubMed: 16944946]

[34]. Cox J, Mann M, MaxQuant enables high peptide identification rates, individualized p.p.b.-range mass accuracies and proteome-wide protein quantification, Nat. Biotechnol. 26 (2008) 1367–1372, 10.1038/nbt.1511. [PubMed: 19029910]

[35]. Maere S, Heymans K, Kuiper M, BiNGO: a Cytoscape plugin to assess overrepresentation of gene ontology categories in biological networks, Bioinformatics 21 (2005) 3448–3449, 10.1093/bioinformatics/bti551. [PubMed: 15972284]

[36]. The Gene Ontology Consortium, Gene ontology: tool for the unification of biology, Nat. Genet. 25 (2000) 25–29, 10.1038/75556. [PubMed: 10802651]

[37]. Supek F, Bosnjak M, Skunca N, Smuc T, Bošnjak M, Škunca N, et al. , REVIGO summarizes and visualizes Long lists of gene ontology terms, PLoS One 6 (2011) e21800, , 10.1371/journal.pone.0021800.

[38]. Team RDC, R development Core team R. R: a language and environment for statistical computing. R found, Stat. Comput. 1 (2005) 409, 10.1007/978-3-540-74686-7.

[39]. Emms DM, Kelly S, OrthoFinder: phylogenetic orthology inference for comparative genomics, Genome Biol. 20 (2019) 238, , 10.1186/s13059019-1832-y. [PubMed: 31727128]

[40]. Magarinos MP, Carmona SJ, Crowther GJ, Ralph SA, Roos DS, Shanmugam D, et al. , TDR targets: a chemogenomics resource for neglected diseases, Nucleic Acids Res. 40 (2012) D1118–D1127, 10.1093/nar/gkr1053.

[41]. Koziol U, Costábile A, Domínguez MF, Iriarte A, Alvite G, Kun A, et al. , Developmental expression of high molecular weight tropomyosin isoforms in *Mesocestoides corti*, Mol. Biochem. Parasitol. 175 (2011) 181–191, 10.1016/j.molbiopara.2010.11.009. [PubMed: 21093500]

[42]. Costa CB, Monteiro KM, Teichmann A, da Silva ED, Lorenzatto KR, Cancela M, et al. , Expression of the histone chaperone SET/TAF-Iβ during the strobilation process of *Mesocestoides corti* (Platyhelminthes, Cestoda), Parasitology 142 (2015) 1171–1182, 10.1017/S003118201500030X. [PubMed: 25823644]

[43]. Espinoza I, Gomez CR, Galindo M, Galanti N, Developmental expression pattern of histone H4 gene associated to DNA synthesis in the endoparasitic platyhelminth *Mesocestoides corti*, Gene 386 (2007) 35–41, 10.1016/j.gene.2006.07.028. [PubMed: 17005331]

[44]. Costábile A, Marín M, Castillo E, Spatio-temporal expression of *Mesocestoides corti* McVAL2 during strobilar development, Exp. Parasitol. 181 (2017) 30–39, 10.1016/j.exppara.2017.07.005. [PubMed: 28750771]

[45]. Espinoza I, Galindo M, Bizarro CV, Ferreira HB, Zaha a., Galanti N, Early postlarval development of the endoparasitic platyhelminth Mesocestoides corti: trypsin provokes reversible tegumental damage leading to serum-induced cell proliferation and growth, J. Cell. Physiol. 205 (2005) 211–217, 10.1002/jcp.20382. [PubMed: 15887242]

[46]. Thompson RCA, Biology and systematics of Echinococcus, Adv. Parasitol. 95 (2017) 65–109, 10.1016/bs.apar.2016.07.001. [PubMed: 28131366]

[47]. Koziol U, Domínguez MF, Marín M, Kun A, Castillo E, Stem cell proliferation during in vitro development of the model cestode *Mesocestoides corti* from larva to adult worm, Front. Zool. 7 (2010) 22, 10.1186/1742-9994-7-22. [PubMed: 20626875]

[48]. Basika T, Macchiaroli N, Cucher M, Espínola S, Kamenetzky L, Zaha A, et al. , Identification and profiling of microRNAs in two developmental stages of the model cestode parasite *Mesocestoides corti*, Mol. Biochem. Parasitol. (2016), 10.1016/j.molbiopara.2016.08.004.

[49]. Cui SJ, Xu LL, Zhang T, Xu M, Yao J, Fang CY, et al. , Proteomic characterization of larval and adult developmental stages in *Echinococcus granulosus* reveals novel insight into host-parasite interactions, J. Proteome 84 (2013) 158–175, 10.1016/j.jprot.2013.04.013.

[50]. dos Santos G.B., Monteiro KM, da Silva ED, Battistella ME, Ferreira HB, Zaha A, Excretory/secretory products in the *Echinococcus granulosus* metacestode: is the intermediate host complacent with infection caused by the larval form of the parasite? Int. J. Parasitol. 46 (2016) 843–856, 10.1016/j.ijpara.2016.07.009. [PubMed: 27771257]

[51]. Vendelova E, Camargo de Lima J, Lorenzatto KR, Monteiro KM, Mueller T, Veepaschit J, et al. , Proteomic analysis of excretory-secretory products of *Mesocestoides corti* Metacestodes reveals potential suppressors of dendritic cell functions, PLoS Negl. Trop. Dis. 10 (2016) e0005061, , 10.1371/journal.pntd.0005061.

[52]. Kramer G, Kasper PT, de Jong L, de Koster CG, Gevaert K, Vandekerckhove J (Eds.), Quantitation of Newly Synthesized Proteins by Pulse Labeling with Azidohomoalanine, vol. 753, Humana Press, Totowa, NJ, 2011, pp. 169–181, , 10.1007/978-1-61779-148-2_12.

[53]. Ullrich M, Liang V, Chew YL, Banister S, Song X, Zaw T, et al. , Bio-orthogonal labeling as a tool to visualize and identify newly synthesized proteins in *Caenorhabditis elegans*, Nat. Protoc. 9 (2014) 2237–2255, 10.1038/nprot.2014.150. [PubMed: 25167056]

[54]. Shen W, Liu H-H, Schiapparelli L, McClatchy D, He H, Yates JR, et al. , Acute synthesis of CPEB is required for plasticity of visual avoidance behavior in Xenopus, Cell Rep. 6 (2014) 737–747, 10.1016/j.celrep.2014.01.024. [PubMed: 24529705]

[55]. McClatchy DB, Ma Y, Liu C, Stein BD, Martínez-Bartolomé S, Vasquez D, et al. , Pulsed Azidohomoalanine Labeling in mammals (PALM) detects changes in liverspecific LKB1 knockout mice, J. Proteome Res. 14 (2015) 4815–4822, 10.1021/acs.jproteome.5b00653. [PubMed: 26445171]

[56]. Glenn WS, Stone SE, Ho SH, Sweredoski MJ, Moradian A, Hess S, et al. , Bioorthogonal noncanonical amino acid tagging (BONCAT) enables time-resolved analysis of protein synthesis in native plant tissue, Plant Physiol. 173 (2017) 1543–1553, 10.1104/pp.16.01762. [PubMed: 28104718]

[57]. Coghlan A, Tyagi R, Cotton JA, Holroyd N, Rosa BA, Tsai IJ, et al. , Comparative genomics of the major parasitic worms, Nat. Genet. 51 (2019) 163–174, 10.1038/s41588-018-0262-1. [PubMed: 30397333]

[58]. Sun M, Long J, Yi Y, Xia W, Importin α-importin β complex mediated nuclear translocation of insulin-like growth factor binding protein-5, Endocr. J. 64 (2017) 963–975, 10.1507/endocrj.ej17-0156. [PubMed: 28835592]

[59]. Wang W, Drosophila Epsin mediates a select endocytic pathway that DSL ligands must enter to activate notch, Development 131 (2004) 5367–5380, 10.1242/dev.01413. [PubMed: 15469974]

[60]. Hemer S, Konrad C, Spiliotis M, Koziol U, Schaack D, Förster S, et al. , Host insulin stimulates *Echinococcus multilocularis* insulin signalling pathways and larval development, BMC Biol. 12 (2014) 5, 10.1186/1741-7007-12-5. [PubMed: 24468049]

[61]. Voronin DA, Kiseleva EV, Functional role of proteins containing ankyrin repeats, Cell Tissue Biol. 2 (2008) 1–12, 10.1134/S1990519X0801001X.

[62]. van der Geer P, Hunter T, Lindberg RA, Receptor protein-tyrosine kinases and their signal transduction pathways, Annu. Rev. Cell Biol. 10 (1994) 251–337, 10.1146/annurev.cb.10.110194.001343. [PubMed: 7888178]

[63]. Pestova TV, Lomakin IB, Lee JH, Choi SK, Dever TE, Hellen CU, The joining of ribosomal subunits in eukaryotes requires eIF5B, Nature 403 (2000) 332–335, 10.1038/35002118. [PubMed: 10659855]

[64]. Lee S, Truesdell SS, Bukhari SIA, Lee JH, LeTonqueze O, Vasudevan S, Upregulation of eIF5B controls cell-cycle arrest and specific developmental stages, Proc. Natl. Acad. Sci. 111 (2014) E4315–E4322, 10.1073/pnas.1320477111.

[65]. Wen C, Levitan D, Li X, Greenwald I, Spr-2, a suppressor of the egg-laying defect caused by loss of sel-12 presenilin in *Caenorhabditis elegans*, is a member of the SET protein subfamily, Proc. Natl. Acad. Sci. 97 (2000) 14524–14529, 10.1073/pnas.011446498.

[66]. Lee J, Bandyopadhyay J, Lee J. Il, Cho I, Park D, Cho JH, A role for Peroxidasin PXN-1 in aspects of *C. elegans* development, Mol. Cell 38 (2015) 51–57, 10.14348/molcells.2015.2202.

[67]. Turner BE, Basecke SM, Bazan GC, Dodge ES, Haire CM, Heussman DJ, et al. , Proteomic identification of germline proteins in Caenorhabditis elegans, Worm 4 (2015) e1008903, , 10.1080/21624054.2015.1008903.

[68]. Chen MJ, Dixon JE, Manning G, Genomics and evolution of protein phosphatases, Sci. Signal. 10 (2017) eaag1796, , 10.1126/scisignal.aag1796.

[69]. Berry M, Gehring W, Phosphorylation status of the SCR homeodomain determines its functional activity: essential role for protein phosphatase 2A,B, EMBO J. 19 (2000) 2946–2957, 10.1093/emboj/19.12.2946. [PubMed: 10856239]

[70]. Mayer-Jaekel RE, Baumgartner S, Bilbe G, Ohkura H, Glover DM, Hemmings B a, Molecular cloning and developmental expression of the catalytic and 65-kDa regulatory subunits of protein phosphatase 2A in Drosophila, Mol. Biol. Cell 3 (1992) 287–298, 10.1091/mbc.3.3.287. [PubMed: 1320961]

[71]. Nourry C, Grant SGN, Borg J-P, PDZ Domain Proteins: Plug and Play!, Sci. Signal. 2003 (2003), 10.1126/scisignal.1792003re7re7-re7.

[72]. Jeleń F, Oleksy A, Smietana K, Otlewski J, PDZ domains - common players in the cell signaling, Acta Biochim. Pol. 50 (2003) 985–1017. [PubMed: 14739991]

[73]. Shen Z, Zhang X, Chai Y, Zhu Z, Yi P, Feng G, et al. , Conditional knockouts generated by engineered CRISPR-Cas9 endonuclease reveal the roles of Coronin in *C. elegans* neural development, Dev. Cell 30 (2014) 625–636, 10.1016/j.devcel.2014.07.017. [PubMed: 25155554]

[74]. Guichet A, Essential role of endophilin a in synaptic vesicle budding at the Drosophila neuromuscular junction, EMBO J. 21 (2002) 1661–1672, 10.1093/emboj/21.7.1661. [PubMed: 11927550]

[75]. Iden S, Collard JG, Crosstalk between small GTPases and polarity proteins in cell polarization, Nat. Rev. Mol. Cell Biol. 9 (2008) 846–859, 10.1038/nrm2521. [PubMed: 18946474]

[76]. Paludo GP, Thompson CE, Miyamoto KN, Guedes RLM, Zaha A, de Vasconcelos ATR, et al. , Cestode strobilation: prediction of developmental genes and pathways, BMC Genomics 21 (2020) 487, , 10.1186/s12864-020-06878-3. [PubMed: 32677885]

[77]. Brown N, In Silico Medicinal Chemistry, Royal Society of Chemistry, Cambridge, 2015, 10.1039/9781782622604.

[78]. Baycin-Hizal D, Tabb DL, Chaerkady R, Chen L, Lewis NE, Nagarajan H, et al. , Proteomic analysis of Chinese hamster ovary cells, J. Proteome Res. 11 (2012) 5265–5276, 10.1021/pr300476w. [PubMed: 22971049]

[79]. Wang X, Li D, Song S, Zhang Y, Li Y, Wang X, et al. , Combined transcriptomics and proteomics forecast analysis for potential genes regulating the Columbian plumage color in chickens, PLoS One 14 (2019) e0210850, , 10.1371/journal.pone.0210850.

[80]. Monteiro KM, De Carvalho MO, Zaha A, Ferreira HB, Proteomic analysis of the *Echinococcus granulosus* metacestode during infection of its intermediate host, Proteomics 10 (2010) 1985–1999, 10.1002/pmic.200900506. [PubMed: 20217864]

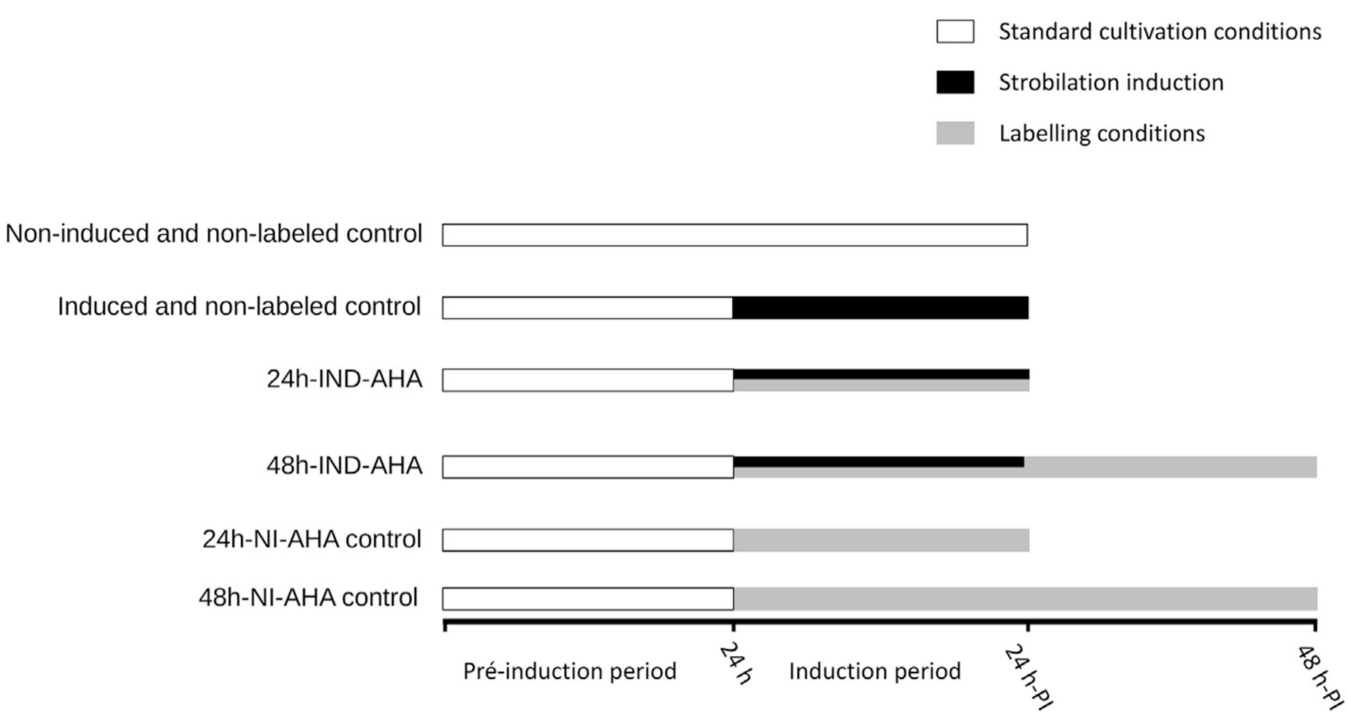

Fig. 1.

Overall experimental design. The different experimental procedures to which the different TT samples were submitted are shown in a timeline, as indicated. Details of the experimental procedures are described in the text.

Fig. 2.

DIC microscopy images of *M. corti* morphology during the initial steps of strobilation. (A) Lateral view of a thetrathyridium, non-induced control. (B) After 24 h of induction of strobilation, a TT shows a more evident constriction behind the suckers (arrowhead). (C) Lateral view of a TT 48 h after induction of strobilation with a clearer separation of the scolex region, with the suckers. Scale bars = 100 μm (A and B) or 500 μm (C).

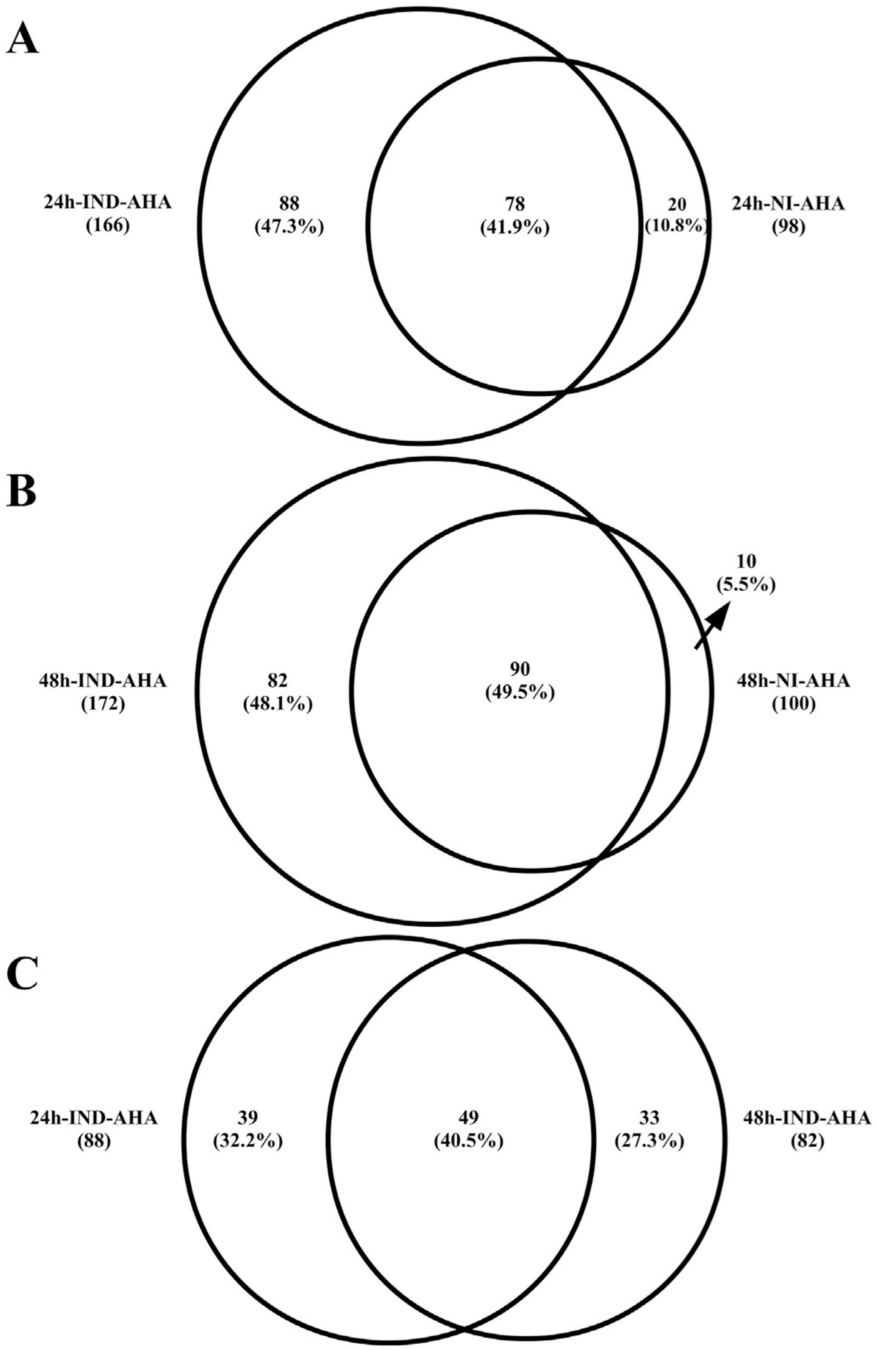

Fig. 3.

Overview of the proteins identified in the NS protein samples. Venn diagrams of (A) 24 h-IND-AHA and 24 h-NI-AHA; (B) 48 h-IND-AHA and 48 h-NI-AHA; and (C) proteins exclusively detected in 24 h-IND-AHA and 48 h-IND-AHA. Total numbers of proteins are indicated for each sample outside the diagram and the numbers and percentages of proteins exclusively detected in each sample or shared between them are indicated within the diagram.

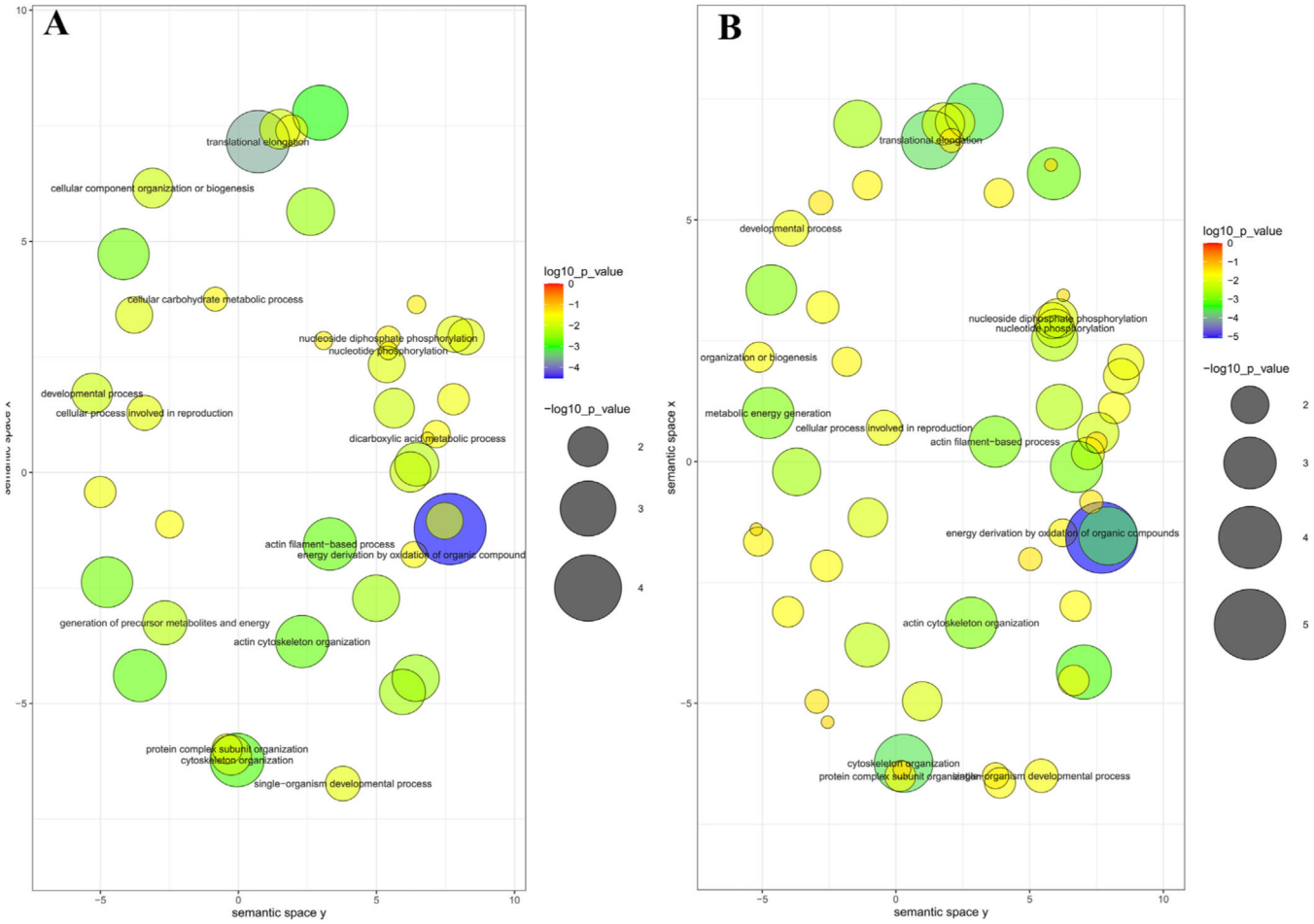

Fig. 4.

Summarized functional classification of differentially abundant proteins identified in the 24 h-IND-AHA and 48 h-IND-AHA samples. Scatterplot view of REVIGO category clusters (summarizing related functional GO-terms) enriched in 24 h-IND-AHA (A) and 48 h-IND-AHA (B). Only “biological process” categories are shown. Color and size are proportional to the *p*-value (larger spheres and cooler colors indicate more significant *p*-values, according to the scale). For each cluster, a representative term of the semantically similar terms is shown. Similarity among GO terms was calculated using SimRel (default allowed similarity = 0.7).

Table 1

List of AHA-labeled proteins exclusively detected in 24 h-ID-AHA samples. The NSAF values in the different biological replicates (Rep1, 2, and 3) are shown for each detected protein

		NSAF[b]		
Accession number [a]	**Protein name**	**Rep1**	**Rep2**	**Rep3**
MCOS_0000701001-mRNA-1	26S protease regulatory subunit 8	0.0015767	0.0018604	0.00082822
MCOS_0000050401-mRNA-1	26S proteasome non-ATPase regulatory subunit 7	0.001018	0.0016816	0.0010695
MCOS_0000934301-mRNA-1	40S ribosomal protein S3	0.0014739	0.001739	0
MCOS_0000947501-mRNA-1	40S ribosomal protein SA	0.0012417	0	0.0009784
MCOS_0000541701-mRNA-1	60S acidic ribosomal protein P0	0.0010627	0.0015046	0
MCOS_0000779901-mRNA-1	Acidic leucine-rich nuclear phosphoprotein 32 family member A	0.0014562	0.00082469	0
MCOS_0000750401-mRNA-1	Actin-like protein 53D	0.0016077	0.0021679	0.0014477
MCOS_0000108001-mRNA-1	Adenylosuccinate lyase	0.00035238	0.00033262	0
MCOS_0000545001-mRNA-1	Alanine aminotransferase, putative	0	0.0011814	0.00075134
MCOS_0000415001-mRNA-1	AMP-dependent synthetase/ligase domain-containing protein	0.00052314	0.0012345	0.0010992
MCOS_0000585301-mRNA-1	Ankyrin repeat-containing domain-containing protein	0.00018012	0.00012752	0
MCOS_0000027301-mRNA-1	AP complex subunit beta	0.00076966	0.00040361	0.00035937
MCOS_0000001401-mRNA-1	Charged multivesicular body protein 2a	0.0014934	0	0.0031378
MCOS_0000359501-mRNA-1	Cysteine–tRNA ligase, cytoplasmic	0.00078993	0.00053259	0.00059277
MCOS_0000097701-mRNA-1	DNA repair protein	0.0007082	0.00089131	0.00124
MCOS_0000022501-mRNA-1	Dynein light chain, type 1/2 family-containing protein	0.0033564	0.0031681	0.0044076
MCOS_0000643001-mRNA-1	Dynein light chain, type 1/2 family-containing protein	0.0050147	0.0052068	0.0047415
MCOS_0000193901-mRNA-1	Epsin-like, N-terminal domain-containing protein	0	0.0008938	0.000829
MCOS_0000818001-mRNA-1	Eukaryotic translation initiation factor 5B	0.00048262	0.00027333	0
MCOS_0000970501-mRNA-1	F-actin-capping protein subunit beta	0.0009313	0.0011721	0
MCOS_0000571301-mRNA-1	Hepatocyte growth factor-regulated tyrosine kinase substrate	0.00059058	0.00097555	0.00077556
MCOS_0000135301-mRNA-1	Importin subunit alpha	0.00095941	0	0.0011759
MCOS_0000105501-mRNA-1	Innexin	0.00048428	0.00063996	0
MCOS_0000915001-mRNA-1	JYalpha	0.0018541	0.0019759	0.0020106
MCOS_0000038401-mRNA-1	Kinesin heavy chain	0.00055703	0.00030045	0.0006688

		NSAF[b]		
Accession number [a]	**Protein name**	**Rep1**	**Rep2**	**Rep3**
MCOS_0001039101-mRNA-1	Kinesin light chain 3	0	0.0018078	0.001006
MCOS_0000619501-mRNA-1	Non-lysosomal glucosylceramidase	0.00043416	0.00049177	0.00036489
MCOS_0000560801-mRNA-1	Probable myosin regulatory light chain	0.0031388	0.0022221	0.0037098
MCOS_0000643501-mRNA-1	Protein disulfide-isomerase A6	0.00094585	0.0019642	0.00079495
MCOS_0000862701-mRNA-1	Protein DLI-1	0.00045893	0	0.00032142
MCOS_0000809001-mRNA-1	Protein kinase-like domain-containing protein	0.0016433	0.00044319	0.0012332
MCOS_0001022801-mRNA-1	Protein TKT-1	0	0.0011483	0.000852
MCOS_0000511101-mRNA-1	Protein VPS-4	0.0011583	0.0012756	0.00040562
MCOS_0000635901-mRNA-1	Putative importin 7	0.0003183	0.00075113	0
MCOS_0000154601-mRNA-1	Putative synaptosomal associated protein	0.00036807	0.00052114	0
MCOS_0000864201-mRNA-1	T-complex protein 1 subunit gamma	0.0011006	0.0010389	0.0011563
MCOS_0000830701-mRNA-1	Trypsin-like cysteine/serine peptidase domain-containing protein	0.0015347	0.0011267	0.0017914
MCOS_0000014001-mRNA-1	UBA-like domain-containing protein	0.0017896	0.0010859	0.00094003
MCOS_0000691901-mRNA-1	UDP-glucose 6-dehydrogenase	0.00072745	0.00103	0

[a] According to *M. corti* genome assembly version 1.0.4 annotation, available at the WormBase ParaSite (https://parasite.wormbase.org/Mesocestoides_corti_prjeb510/Info/Index/). Helminth Genomes Consortium.

[b] NSAF, normalized espectral abundance factor.

J Proteomics. Author manuscript; available in PMC 2023 September 08.

Table 2

List of AHA-labeled proteins detected both in 24 h-IND-AHA and 48 h-IND-AHA samples. The NSAF values in the different biological replicates (Rep1, 2, and 3) are shown for each detected protein.

		NSAF[b]					
		24 h-IND-AHA			48 h-IND-AHA		
Accession number[a]	**Protein name**	**Rep1**	**Rep2**	**Rep3**	**Rep1**	**Rep2**	**Rep3**
MCOS_0000027001-mRNA-1	1.4-alpha-glucan-branching enzyme	0.0002411	0.00045517	0	0.000232	0.00063	0
MCOS_0000611301-mRNA-1	40S ribosomal protein S3a	0.0016488	0.0018676	0.0017322	0.001583	0	0.00175
MCOS_0000350901-mRNA-1	Adducin-related protein 1	0.00022332	0	0.00046922	0	0.00035	0.000592
MCOS_0000633601-mRNA-1	Adenylate kinase isoenzyme 1	0.0026904	0.0021163	0	0	0.001874	0.001428
MCOS_0000747801-mRNA-1	Annexin	0.001066	0.0015093	0	0.00128	0.001114	0.00198
MCOS_0000094701-mRNA-1	Chloride intracellular channel exc-4	0.0012988	0.0015325	0	0	0.001357	0.001723
MCOS_0000543301-mRNA-1	Coatomer subunit gamma	0.00083177	0.00052342	0.00077674	0.000621	0.000483	0.000785
MCOS_0000033601-mRNA-1	Elongation factor Tu, mitochondrial	0.00076869	0.0010884	0.00080757	0.001107	0.001205	0.001428
MCOS_0000370501-mRNA-1	Eukaryotic initiation factor 4A	0	0.0010178	0.0004531	0	0.001126	0.000915
MCOS_0000013401-mRNA-1	FAA4 Long-chain-fatty-acid–CoA ligase 4	0.00095223	0.0010986	0.001445	0.001727	0.001216	0.001235
MCOS_0000381601-mRNA-1	Ferritin	0.0034291	0.002312	0.0025732	0.002352	0.002559	0.002079
MCOS_0000453001-mRNA-1	Glutathione S-transferase, C-terminal-like domain-containing protein	0.0073404	0.0037793	0.0049074	0.007049	0.006274	0
MCOS_0001023101-mRNA-1	Glycogen debranching enzyme	0.00029701	0.00037381	0	0.000475	0.000517	0.00063
MCOS_0000780101-mRNA-1	HEAT, type 2 repeat-containing protein	0.00074232	0.00093425	0	0.000832	0.000517	0.000919
MCOS_0000366201-mRNA-1	Hypothetical protein	0.00054818	0.00062092	0.00069108	0.000842	0.000573	0.000814
MCOS_0000375101-mRNA-1	Hypothetical protein	0.00080203	0.00037853	0.00098303	0.001027	0.000698	0
MCOS_0000895701-mRNA-1	Hypothetical protein	0.00043879	0.00023667	0.00039512	0.000421	0.000131	0.000333
MCOS_0000471201-mRNA-1	JYalpha	0.0010335	0.00078044	0.0010858	0.000794	0.00108	0.001316
MCOS_0000562501-mRNA-1	Lysosomal alpha-glucosidase	0.00085222	0.0008938	0.00069636	0.001	0.000692	0.000603
MCOS_0000811801-mRNA-1	Mannose-1-phosphate guanyltransferase	0.001378	0.0013007	0.0012064	0	0.00072	0.000975
MCOS_0000780001-mRNA-1	Mitochondrial import receptor subunit TOM70	0.00067475	0.00076429	0.0005671	0.000518	0.000282	0.001289
MCOS_0000623101-mRNA-1	Mitochondrial-processing peptidase subunit beta	0.00067394	0.00095422	0.00070802	0.000518	0.000422	0.000429
MCOS_0000372201-mRNA-1	NAD(P)-binding domain-containing protein	0.0047522	0.0052333	0.0041605	0.004564	0.003309	0.003362
MCOS_0000737601-mRNA-1	Nucleoside diphosphate kinase	0.0045079	0.0038296	0.0042623	0	0.004238	0.004784

		NSAF[b]					
		24 h-IND-AHA			48 h-IND-AHA		
Accession number[a]	Protein name	Rep1	Rep2	Rep3	Rep1	Rep2	Rep3
MCOS_0000203401-mRNA-1	Peroxidasin	0.00038522	0.00024241	0	0.000555	0.000268	0.000204
MCOS_0000365801-mRNA-1	Probable 26S protease regulatory subunit 10B	0.00085604	0.0012121	0.00089933	0	0.000894	0.00159
MCOS_0000249901-mRNA-1	Probable aconitate hydratase. Mitochondrial	0.00027786	0.00078684	0	0	0.000581	0.000885
MCOS_0000131501-mRNA-1	Probable arginine-tRNA ligase, cytoplasmic	0.0017161	0.0013706	0.00083209	0.000887	0.000414	0.000981
MCOS_0000097201-mRNA-1	Probable tubulin polyglutamylase TTLL9	0.00053301	0.00060374	0.00067196	0.000409	0.000445	0
MCOS_0000790801-mRNA-1	Prolyl endopeptidase	0.00084627	0.00045646	0.00076206	0.000813	0.000758	0.001155
MCOS_0000577001-mRNA-1	Protein MAX-2	0.00090158	0.0011914	0.0015155	0.001558	0.000753	0
MCOS_0000675001-mRNA-1	Protein PLST-1	0	0.00038927	0.00021663	0.00033	0	0.000365
MCOS_0000084501-mRNA-1	Protein RME-1	0.00060319	0.00085404	0	0.000579	0.00063	0.0008
MCOS_0000468301-mRNA-1	P-type ATPase, A domain-containing protein	0.0029999	0.0021238	0.0027577	0.002521	0.002742	0.003184
MCOS_0000853301-mRNA-1	Purine nucleoside phosphorylase	0.0012542	0.0011839	0.00075293	0.000688	0.000936	0.001521
MCOS_0001033901-mRNA-1	Putative 40s ribosomal protein S10	0.0042911	0.0030378	0.003381	0.002575	0.001681	0.004554
MCOS_0000788301-mRNA-1	Putative 60s acidic ribosomal protein P2	0.0027786	0	0.0029191	0.00467	0	0.004423
MCOS_0000510101-mRNA-1	Putative inorganic pyrophosphatase	0.0017438	0.001646	0	0.00067	0.002915	0.001851
MCOS_0000203201-mRNA-1	Putative microtubule-associated protein	0.00048016	0.00045323	0	0	0.000167	0.00051
MCOS_0000573501-mRNA-1	Rab-binding domain FIP-RBD-containing protein	0.0010029	0.0011834	0.0026341	0.000482	0.000524	0.000798
MCOS_0000705401-mRNA-1	Retinaldehyde binding protein-related	0	0.0019354	0.001436	0.000438	0.000952	0.001692
MCOS_0000268701-mRNA-1	Suppressor of presenilin-2	0.0016361	0.0012354	0	0	0.001025	0.001389
MCOS_0000562401-mRNA-1	T-complex protein 1 subunit zeta	0.0010845	0.0010237	0.00097661	0	0.000486	0.000822
MCOS_0000946201-mRNA-1	Transcription factor BTF3	0.0016509	0.0015584	0.004047	0	0.002299	0.001168
MCOS_0000751501-mRNA-1	Trypsin-like cysteine/serine peptidase domain-containing protein	0.00095653	0.0010835	0.00080392	0.001102	0.000799	0.000609
MCOS_0000918601-mRNA-1	Tubulin beta-2 chain	0.0020925	0.0017777	0.002638	0.001407	0.00153	0.001777
MCOS_0000247201-mRNA-1	Ubiquitin-conjugating enzyme/RWD-like domain-containing protein	0	0.0034284	0.0038157	0.003488	0.001897	0.00257
MCOS_0000467101-mRNA-1	UDP-glucose 4-epimerase	0.0027119	0	0.0035614	0.005209	0.003541	0.003597
MCOS_0000901501-mRNA-1	UTP–glucose-1-phosphate uridylyltransferase	0.00066863	0.00078891	0.0012293	0.000963	0.000873	0.001419

[a] According to *M. corti* genome assembly version 1.0.4 annotation, available at the WormBase ParaSite (https://parasite.wormbase.org/Mesocestoides_corti_prjeb510/Info/Index/). Helminth Genomes Consortium.

[b] NSAF, normalized espectral abundance factor.

J Proteomics. Author manuscript; available in PMC 2023 September 08.

J Proteomics. Author manuscript; available in PMC 2023 September 08.

Table 3

List of AHA-labeled proteins exclusively detected in 48 h-ID-AHA samples. The NSAF values in the different biological replicates (Rep1, 2, and 3) are shown for each detected protein.

		NSAF [b]		
Accession number [a]	**Protein name**	**Rep1**	**Rep2**	**Rep3**
MCOS_0000228701-mRNA-1	60S acidic ribosomal protein P1	0.0033354	0.0043538	0.004423
MCOS_0000378101-mRNA-1	6-phosphogluconate dehydrogenase. Decarboxylating	0.0031045	0.0024122	0.0029406
MCOS_0000129601-mRNA-1	Adducin-related protein 1	0.00088323	0.00054901	0.00055773
MCOS_0000381901-mRNA-1	Aldo-keto reductase family 1 member C-like protein 1	0.00051265	0.00027883	0.00028326
MCOS_0000338601-mRNA-1	Calnexin	0.0011016	0.0011983	0.00076086
MCOS_0000083501-mRNA-1	Cell polarity protein	0.00010559	0.000057429	0
MCOS_0000357601-mRNA-1	Charged multivesicular body protein 3	0.0022399	0.0012183	0.0016502
MCOS_0000025901-mRNA-1	Concanavalin A-like lectin/glucanase, subgroup domain-containing protein	0.00019947	0	0.00011021
MCOS_0000678801-mRNA-1	Coronin	0	0.00075278	0.00091769
MCOS_0000359801-mRNA-1	Cysteine–tRNA ligase, cytoplasmic	0.0003251	0.00058939	0.00071851
MCOS_0000880201-mRNA-1	Domain of unknown function DUF3421 domain-containing protein	0.0013971	0.0015198	0
MCOS_0000675401-mRNA-1	Endophilin-A	0	0.00047595	0.00048351
MCOS_0000865201-mRNA-1	Glutathione S-transferase class-mu 28 kDa isozyme	0.0030711	0.0025055	0.0025453
MCOS_0000861901-mRNA-1	Guanine nucleotide-binding protein subunit beta-1	0.00047872	0.00078112	0.0015871
MCOS_0000159501-mRNA-1	Hypothetical protein	0.0020178	0.0029265	0
MCOS_0000288501-mRNA-1	Hypothetical protein	0	0.00061907	0.00041927
MCOS_0000339801-mRNA-1	Hypoxia upregulated 1	0	0.00018405	0.00028046
MCOS_0000633301-mRNA-1	Mitochondrial-processing peptidase subunit beta	0.00048539	0.00070399	0
MCOS_0000033301-mRNA-1	NAD(P)-binding domain-containing protein	0.00077262	0.0014007	0
MCOS_0000307601-mRNA-1	NAD-dependent malic enzyme, mitochondrial	0	0.0026625	0.0027048
MCOS_0000215601-mRNA-1	PDZ domain-containing protein	0	0.0023297	0.0018933
MCOS_0000819001-mRNA-1	Probable protein phosphatase 2C	0.00078468	0.00048775	0.0004955
MCOS_0000911901-mRNA-1	Protein ROP	0	0.00037301	0.00088418
MCOS_0000940301-mRNA-1	Putative aspartyl-tRNA synthetase	0.00095185	0.0005177	0
MCOS_0000188301-mRNA-1	Putative sodium/potassium-transporting ATPase subunit beta	0	0.0028957	0.0021013
MCOS_0000194401-mRNA-1	Pyruvate dehydrogenase E1 component subunit beta, mitochondrial	0.0011303	0.00073773	0.00049963

		NSAF [b]		
Accession number [a]	**Protein name**	**Rep1**	**Rep2**	**Rep3**
MCOS_0000203301-mRNA-1	Saposin-related	0.00031544	0.00017156	0.00043573
MCOS_0000008301-mRNA-1	Serine/threonine-protein phosphatase PP2A 65 kDa regulatory subunit	0.00054803	0	0.0010598
MCOS_0000041101-mRNA-1	Subfamily M16B non-peptidase homologue	0.0010194	0.00055445	0.00056326
MCOS_0000985401-mRNA-1	Transketolase-like protein 2	0.00065897	0.00071682	0.0014564
MCOS_0000436001-mRNA-1	Tubulin alpha-4A chain	0.00090225	0.00098145	0.00079764
MCOS_0000552901-mRNA-1	Ubiquitin carboxyl-terminal hydrolase	0.00031271	0	0.00025917
MCOS_0000558101-mRNA-1	UDP-glucose 6-dehydrogenase	0.00096502	0.00034991	0

[a] According to *M. corti* genome assembly version 1.0.4 annotation, available at the WormBase ParaSite (https://parasite.wormbase.org/Mesocestoides_corti_prjeb510/Info/Index/). Helminth Genomes Consortium.

[b] NSAF, normalized espectral abundance factor.